OPTIMIZED FIBER STEERING AND LAYER STACKING FOR ELASTICALLY TAILORED, DAMAGE TOLERANT LAMINATES

W. Liu, R. Butler* and A.T. Rhead
Composites Research Unit, Department of Mechanical Engineering,
University of Bath, Bath, UK
* Corresponding author (R.Butler@bath.ac.uk)

Keywords: *Optimization, variable angle tows, buckling, compression after impact, damage tolerance*

Abstract

A combined minimum-mass optimization strategy for Variable Angle Tow (VAT) panels subject to buckling and damage tolerance constraints is presented. The manufacturing process of Continuous Tow Shearing (CTS) is employed to form the laminates which have variable thickness due to tow shear deformation of dry tows. The panels under compression load are modeled using an infinite strip method to predict the panel buckling load and an efficient damage tolerance model is applied to obtain the threshold strains for crack propagation at delamination interfaces. Straight fiber ±45° plies show a good compromise between damage tolerance and buckling capacity by a trade-off study. These plies are added to the surfaces of the optimum buckling design to improve the Damage Tolerant (DT) strength in the highly-stressed area near the panel boundaries. This buckling/DT laminate is re-optimized with buckling and damage tolerance constraints. The results show that the damage tolerant strength of buckling/DT laminate improves by up to 71% with 6% weight saving compared with the laminate optimized with only buckling constraints. Hence, the proposed optimization strategy provides structurally efficient solutions for optimum design of CTS panels with buckling and damage tolerance constraints.

1 Introduction

Variable angle tows have the potential to significantly improve the compressive capacity of CFRP composite panels. For example, buckling performance can be improved by stiffness redistribution towards panel boundaries [1]. Compared with conventional straight fibers, VAT composites allow the designer freedom to vary the fiber angle as a function of position throughout the structure, resulting in variable stiffness and strength without adding additional plies [2-4].

In order to bring VAT panels from conceptual to application scenarios, a variety of manufacturing techniques have been developed. Conventional Automated Fiber Placement (AFP) techniques use tow head turning to control the angle change. Blom et al [5] reduced the tow overlap and tow cut-off to improve the quality of the VAT panels.

Two methods can be used to lay tows in terms of a reference tow path when AFP is applied; parallel paths and shifted (similar) paths. The advantage of parallel paths is that no gaps or overlaps will occur between tows, resulting in a laminate with uniform thickness and (theoretically) without any defects. However, the disadvantage is that the steering radius of parallel tows may result in violation of the maximum allowable tow curvature. A geometric singularity can also occur. Shifted paths keep each tow path the same as the reference tow path, resulting in tow overlaps and/or tow gaps. The tow overlap case occurs when two adjacent courses move closer to eliminate the gap. An overlap (or gap) produces local thickening (or thinning) which is accompanied by localized out-of-plane fiber waviness as well as locally resin-rich areas, which may decrease structural strength. Tow cutting can be used to reduce tow gaps and keep the panel mass as low as the one obtained from the design stage, but produces fiber discontinuity. For both parallel and shifted cases, fiber wrinkling is caused by localized buckling in the internal radius of AFP tows subject to in-plane bending. This limits the minimum radius

of steering to 635mm (1778mm) for a 3.175mm (6.35mm) tow width [6].

A collaborative project between the universities of Bristol and Bath has developed a Continuous Tow Shearing (CTS) technique [7] for fiber placement, which uses the deformable characteristic of dry tows in shear and can significantly reduce process-induced defects compared with AFP techniques, which use in-plane bending deformation. In addition, the design flexibility is increased by reducing the minimum radius of curvature of each tow path to around 30mm. The CTS technique offers smooth thickness distribution rather than the discontinuous thickness caused by tow overlapping in AFP. CTS also reduces process-induced defects such as fiber wrinkling, resin rich areas and fiber discontinuity compared with conventional AFP techniques, which use in-plane bending to steer tows. In contrast, the CTS technique uses dry tows combined with an in-situ impregnation to provide shearing capability and prevent the fiber splitting.

However, damage tolerance of panels built using variable angle tows has not yet been considered in the design stage. Lopes et al [8] have simulated impact tests for straight fiber and VAT laminates to study crack propagation of VAT panels. Rhead et al [9] have tested such coupons designed without consideration of damage tolerance, showing the highly stressed regions created along the panel boundaries may not be able to tolerate damage.

A combined optimization strategy for minimum mass design satisfying both buckling and damage tolerance constraints is proposed for CTS panels. A computationally efficient damage tolerance model [10] is applied to predict the threshold of failure strain. The idea of the combined optimization is based on blended layer stacking of CTS layers and straight fiber layers to improve the damage tolerance of the highly-stressed area near the panel boundaries.

2 CTS Manufacture and Optimization

During the CTS manufacturing process, the tow is sheared and the thickness is changed according to the shear angle. Assuming the fiber volume of the tow element is not changed, the thickness change of the tow element before and after the shear deformation is shown in Fig. 1. The tow shearing angle is defined as β and the angle θ is the tow angle defined in the strip model for panel buckling. The relationship of the two angles is $\theta = 90° - \beta$.

The change of the sheared tow thickness t according to the average tow thickness t_0 before shearing and the tow angle θ is given by

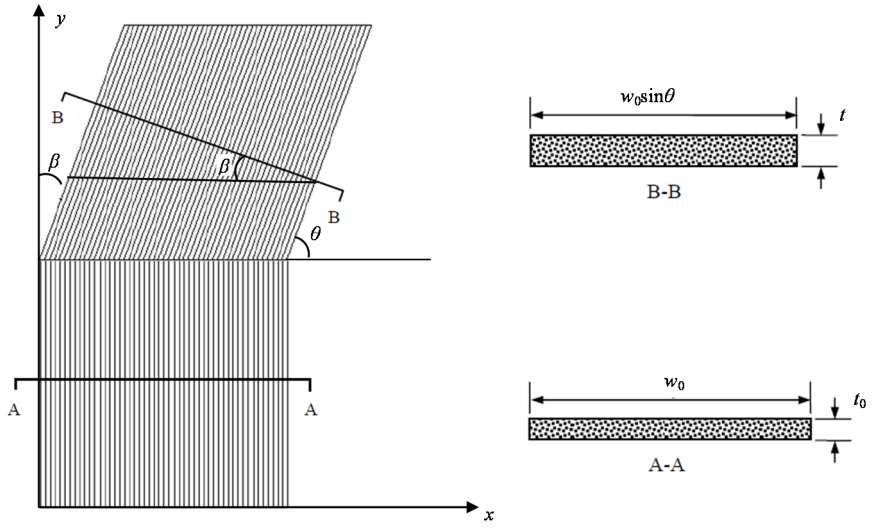

Fig. 1 Thickness change of tow element due to shear deformation in CTS method. The tow element with cross section A-A shows tow thickness before shear, whereas B-B shows the thickness change after shear.

$$t = \frac{t_0}{\sin\theta} \qquad (1)$$

which is deducted from $t_0 w_0 = tw$ and $w = w_0 \sin\theta$ due to the unchanged fiber volume of the tow element, where w_0 and w are the tow width before and after shearing.

The formula is singular when $\theta = 0°$. Therefore, θ will not be allowed to be equal to zero degrees for manufacturability reasons. In practice, the tow angle which the tow head of the prototype CTS machine can achieve is $15° \le \theta \le 90°$.

The structure considered in this work is a laminated flat panel of length L, and width B. The dimensions and notation are shown in Fig. 2. The panel is made of 8 layers of steered unidirectional carbon fibers in an epoxy resin with a fully uncoupled stacking sequence of [θ/-θ/-θ/θ/-θ/θ/θ/-θ]. The reference fiber paths vary along the y axis, i.e. $\theta = \theta(y)$, which means that the tow shifting direction is along the x axis. Note that the solid curves in Fig. 1 indicate $+\theta$ paths, whereas the dashed curves indicate $-\theta$ paths.

Gürdal et al. [3] studied two cases of tow paths which linearly vary along the longitudinal x direction or the transverse y direction. They showed that, due to redistribution of the longitudinal compressive load P_x, fiber angle variation in the y direction is more efficient than variation in the x direction in the case of initial buckling. In this paper therefore, we focus on variation in the direction transverse to load, in order to achieve the best structural efficiency whilst retaining prismatic conditions. We apply an efficient optimization strategy for design of VAT panels with minimum mass whilst satisfying buckling load and CTS manufacturing constraints. We use a gradient-based method, which suits the continuity of tow paths. Local optima can be readily avoided by selecting different starting points covering all the design space. The optimization treats the fiber angles as design variables and VIPASA [11] buckling analysis is selected, since it suits transverse variation of angle. As VIPASA is fast, requiring 0.1% of FEM computation time, its use in optimization is very efficient.

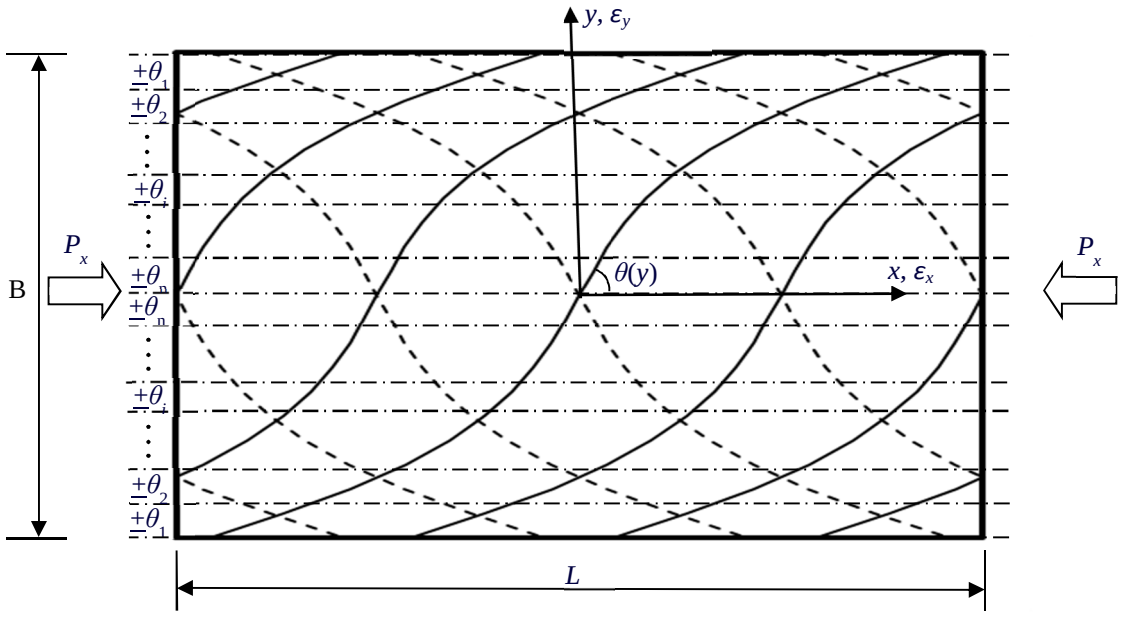

Fig. 2 Fiber path definition of the VAT panel. θ_i is the fiber orientation angle in each strip for a VAT ply. The compressive load P_x is applied as uniform end-shortening ε_x. The transverse strain is indicated by ε_y.

VAT panels are divided into a number of strips of equal width and the fiber angle θ_i of each strip is free to vary whilst satisfying buckling constraints. Anti-symmetry is imposed about the panel centerline, as shown in Fig. 2. The figure illustrates that the fiber path $\theta(y)$ is represented as the fiber angle θ_i in each strip. The number of strips for buckling analyses was checked to ensure mesh convergence whilst maintaining computational efficiency.

3 Damage Tolerance Model

Low energy impact can cause Barely Visible Impact Damage (BVID) in laminates and their residual strength of compression after impact can reduce up to 60%.

A Strip model has been developed that calculates the approximate compressive threshold strain ε_{th}, below which propagation of a delamination will not occur. This strain is given by the equation,

$$\varepsilon_{th} = \varepsilon^C \left(\sqrt{4 + \frac{2G_{IC}}{(\varepsilon^C)^2 A_{11}}} - 1 \right) \tag{2}$$

Here ε^C is the buckling strain of the delaminated sublaminate, A_{11} is the axial stiffness of the sub laminate and G_{IC}, the mode I Strain Energy Release Rate. Threshold strains are calculated at each ply interface from the surface ply to establish the minimum value. This is normally between 10 and 20% of laminate thickness. The method requires an assumed distribution of through-thickness delamination. These are usually approximated as circles of constant diameter d. Straight fiber laminates have previously been optimized to maximize damage tolerance [12] by automatically selecting the best stacking sequences in order to maximize the stress at which buckle-driven propagation of delamination occurs. The optimized designs have been experimentally verified via compression after impact testing [13].

The minimum of Eq. (2) is given by

$$\frac{\partial \varepsilon_{th}}{\partial \varepsilon^C} = 0, \tag{3}$$

at which the following condition is obtained

$$\varepsilon^C = \sqrt{\frac{G_{1C}}{6A_{11}}} \tag{4}$$

Replacing ε^C in Eq (2) by Eq. (4), the minimum threshold strain $\varepsilon_{th,min}$ is then obtained as

$$\varepsilon_{th,min} = \sqrt{\frac{3G_{1C}}{2A_{11}}} \tag{5}$$

Because d is limited by the amount of impact energy required to cause BVID, a maximum diameter d_{max} is applied during the optimization procedure. The buckling strain of the delaminated sub-laminate ε^C can be interpolated from the following equation

$$\varepsilon^C = K \left(\frac{1}{d} \right)^2 \tag{6}$$

where K is a buckling coefficient dependent on the thickness and stacking sequence of the sublaminate. K can be obtained for different interfaces by using the strip program VICONOPT [14] to calculate a single ε^C for a given d with an assumption that the transverse strain, ε_y in Fig. 2 applied on the sublaminate is equal to zero. This causes an extra transverse compression load in the y direction, resulting in conservative values of CTS sublaminate buckling strain ε^C.

Having obtained K, the delamination diameter d at which the minimum threshold strain $\varepsilon_{th,min}$ occurs can be obtained by substituting Eq. (4) into Eq. (6). If this diameter is greater than a maximum diameter d_{max}, this means that the minimum threshold strain $\varepsilon_{th,min}$ cannot be reached within the BVID criterion. In this case d_{max} is used to give the threshold strain.

4 Optimization of Laminates for Damage Tolerance and Buckling Resistance

In this section, an investigation of effects of ply angles on damage tolerance (DT) and buckling resistance is performed to find a good compromise between these two structural design requirements. A combined optimization strategy is described in order to improve damage tolerance of CTS laminates.

Previous studies [15] have shown that, in terms of damage tolerance, fiber angles between 0º and ±40º should be avoided on the surface of laminates owing

to the low strain at which buckling-driven propagation of delamination occurs. This is due to the increased load that is drawn into the sublaminate owing to the high axial stiffness of the plies. Surface plies with fiber angles between ±60º and 90º will, in many cases, exhibit other failure mechanisms instead of buckling-driven propagation. Hence, in terms of maximum damage tolerance, the optimum angle of straight fiber layers, placed at the surface of the laminate, is in the range ±40º to ±60º. To improve DT of CTS panels, ±45º angle plies are added on the top and bottom surfaces of the CTS laminate because these angle plies have good DT and buckling capacity. This is explained in the following three paragraphs.

In order to understand the damage tolerance of plies with variable angle θ, Eq. (2) is used to calculate the critical threshold strain ε_{th} for laminates with stacking sequences $[(\pm\theta)_4]_s$ and $[\pm45/(\pm\theta)_3]_s$, see Fig. 3. (Note that a constant ply thickness of 0.25mm and a circular delamination of 40mm diameter at each ply interface were assumed for M21/T700 material.) It can be seen that the influence of ±45° surface plies is to increase threshold strain when $0° < \theta < 45°$. When θ is approximately 25°, the Poisson's ratio of the laminate is at a maximum value of approximately 1.5. This induces lateral tension in the outer plies, making them very difficult to buckle, and the threshold strain becomes extremely large. In practice, of course, the laminate will fail by an alternative mechanism before this theoretical level of compressive strain is reached.

Figure 4 converts the strain values of Fig. 3 to predictions of strength by applying the effective elastic modulus of each laminate. Although the strength of laminates is limited by the $\theta = 0°$ value, practical application necessitates that $\theta \neq 0°$, in which case the addition of ±45° surface layers always improves strength when $0° < \theta < 45°$.

The buckling load P_x^C for a long, simply-surpported panel of width B can be calculated by the following equation,

$$P_x^c = \frac{\pi^2}{B}\left[2\sqrt{D_{11}D_{22}} + 2(D_{12} + 2D_{33})\right] \qquad (6)$$

where D_{11}, D_{22}, D_{12} and D_{33} are terms from the bending stiffness matrix of the laminate. Figure 5 illustrates the variation of buckling load with different ply angles, showing that 45° plies give the maximum buckling load.

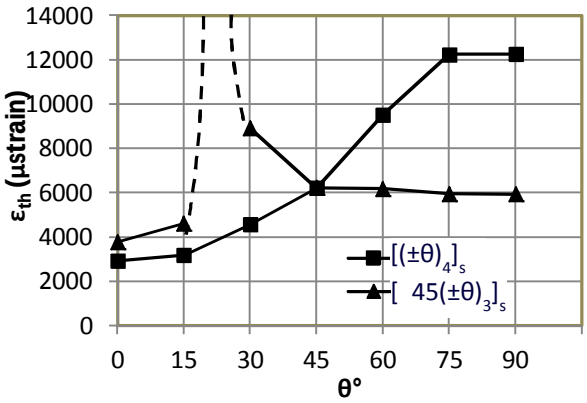

Fig. 3 Damage tolerant threshold strain for $[(\pm\theta)_4]_s$ and $[\pm45/(\pm\theta)_3]_s$ laminates.

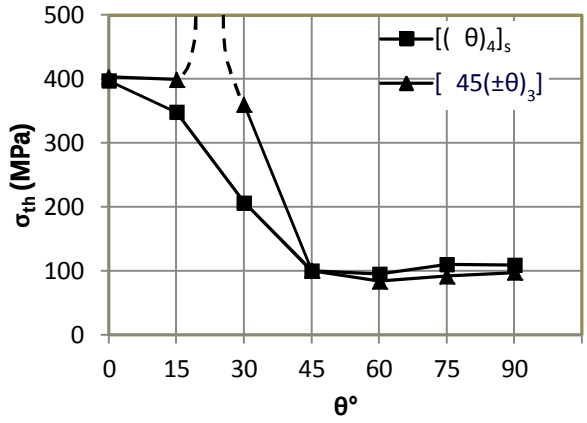

Fig. 4 Damage tolerant threshold strength for $[(\pm\theta)_4]_s$ and $[\pm45/(\pm\theta)_3]_s$ laminates.

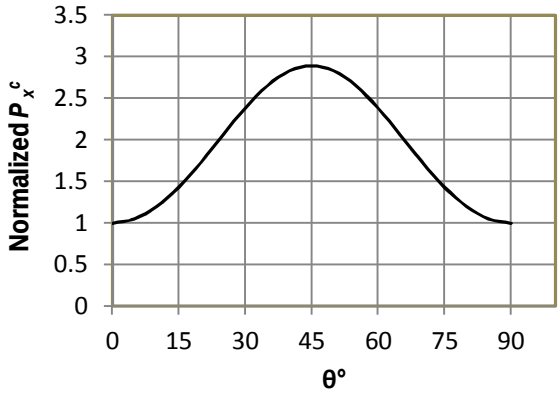

Fig. 5 Normalized buckling load for fiber angle θ.

4.1 Combined Optimization Strategy

A new method that combines the minimum mass optimization of steered CTS fiber laminates for buckling constraints, with the design of surface layers for damage tolerant strength constraints is presented.
The flow of the optimization process is summarized in Fig. 6 and described as follows.

1. *Optimise CTS laminates with buckling constraints for minimum panel mass.*
2. *Analyse damage tolerant strength of the optimum buckling design.*
3. *Add ±45º plies on the surfaces of strips where fiber angle $\theta < 45°$, forming buckling/DT laminates.*
4. *Analyse damage tolerant strength of the buckling/DT laminates.*
5. *Re-optimise buckling/DT laminates with buckling and damage tolerance constraints.*
6. *If there are strips with fiber angle $\theta < 45°$ not covered by ±45º plies, cover these strips with ±45º plies and repeat Step 5 until strips with fiber angle $\theta < 45°$ are all covered.*
7. *Repeat steps 3-7 until convergence.*

Fig. 6 Combined optimization strategy.

In the first step, VICONOPT is used to find optimum ply thickness and fiber angles with minimum panel mass satisfying buckling constraints. In the second step, the damage tolerance model is applied to find the damage tolerance strength of the initial CTS optimum buckling design. According to Eq. (5), the minimum threshold strain $\varepsilon_{th,min}$ is the worst case at each ply interface regardless of the delamination size. The lowest threshold strain is defined as the damage tolerant strain ε_{all} of the initial CTS optimum buckling design. If this ε_{all} is lower than the buckling strain when buckling load is applied, the initial CTS optimum buckling design will not be able to carry the required buckling load, i.e. design load.
In order to improve the damage tolerance of the initial CTS optimum buckling design, and because it has been proved that ±45º plies offers a good compromise between damage tolerance and buckling resistance, during the third step, surface plies of ±45º are added to top and bottom surfaces in regions where damage tolerant strength is not adequate, named as buckling/DT laminates. The damage tolerance model is applied to calculate threshold strains of the buckling/DT laminate at different interfaces and fiber angles. The lowest threshold strain is defined as the damage tolerant strain ε_{all} of the buckling/DT laminate. This value of strain is applied to the next optimization step as a strain constraint.
In the fifth step, the buckling/DT laminate is re-optimized using VICONOPT to satisfy buckling load and damage tolerant strain (ε_{all}) requirement. The number of strips with ±45º plies is adjusted to ensure that the strips with fiber angle $\theta < 45°$ are all covered by repeating Step 5 and 6 for the optimization with increased number of ±45° plies. This process of CTS optimization and damage tolerance design is continued until convergence, at which point the overall laminate design does not change.

5 Design Example and Results

The example presented here is to design a VAT panel of length L = 750mm and width B = 250mm. The material properties are E_{11} = 130GPa, E_{22} = 9.25GPa, G_{12} = 5.1GPa, ν_{12} = 0.36, ρ = 1584kg/m^3 and G_{IC} = 500J/m^2. The thickness of straight fiber (±45°) layers is 0.25 mm. The compressive design load P_x is 250kN, applied as uniform end shortening. The panel is simply supported along all four edges. There are 10 strips used to divide the half width panel, i.e. n = 10, refer to Fig. 2.
The minimum mass optimization of the CTS panel was first performed with buckling constraints using a version of VICONOPT that was been updated for modeling of CTS panels. The optimum results of the fiber path for the bucking optimum design is illustrated in Fig. 7. The fiber angle θ_1 at the edge of the panel is 20°, whereas the fiber angle θ_{10} in the center of the panels is 68°, see Table 1, resulting in the compression load being redistributed to the panel boundaries. For this design, when the stacking sequence has 8 plies as [θ/-θ/-θ/θ/-θ/θ/θ/-θ], the tow thickness t within strips 1 and 2 is above 0.75 mm. This thick stack can induce fiber splitting, which needs to be avoided. Hence, the 16 ply laminate [θ/-θ/-θ/θ/-θ/θ/θ/-θ]$_S$ was used. The buckling strain is 6061 microstrain. The damage tolerance model described in Section 3 was then applied to obtain the

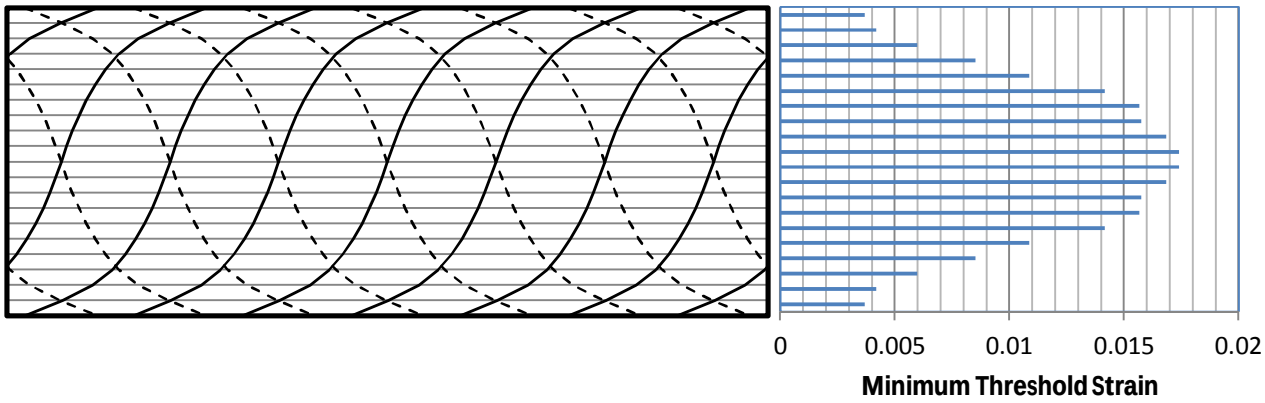

Fig. 7 Fiber path and threshold strain of each strip in optimum buckling (CTS) design.

minimum damage tolerant strain by using Eq. (5). Figure 7 shows these strain values at the first ply interface for each fiber angle θ_i. It can be seen that the lowest threshold strain is 3682 microstrain, indicating that delamination damage in the panel caused by impact or manufacturing defects can propagate before the design load.

Hence, ±45º plies were added on the top and bottom of the buckling design, where the fiber angle of strips has $\theta_i < 45°$ to improve the damage tolerance. Therefore, the 3 strips close to the panel edges were covered by ±45º plies. The damage tolerance model was applied to analyze the buckling/DT laminates to obtain the lowest threshold strain at each interface for each fiber angle. At the first and second ply interfaces where the sublaminates are a single 45° ply and ±45º plies, respectively, the minimum threshold strains $\varepsilon_{th,min}$ are 8430 and 5982 microstrain, respectively. For the third interface where the sublaminates include a CTS ply, the minimum threshold strains and the corresponding sublaminate buckling strain ε^C were calculated. Here, the delamination diameters obtained from Eq. (6), are all above 50 mm. Therefore, the maximum diameter d_{max} = 30 mm was applied. Table 2 presents the results of these threshold strains at the third interface for the fiber angles $\theta_i < 45°$, showing that the critical damage tolerant strain is 5401 microstrain when $\theta_2 = 24.4°$. This strain value was then applied as a strain allowable ε_{all} to the minimum mass optimization with buckling and damage tolerant strength constraints.

Table 2 Threshold strain of buckling design with ±45º surface plies.

Strip no.	1	2	3
Buckling/DT plies	±45/20.5	±45/24.4	±45/35.0
ε_{th} (με)[1]	5622	5401	5496

[1]The delamination diameter d is 30mm.

During the re-optimization step, the optimization cycle described in Steps 5 and 6 in Section 4 was performed to find an adequate number of strips

Table 1 Comparison of fiber angle for optimum buckling design and buckling/DT design. Note that tow thickness of each strip is given by Eq. (1).

	Strip no.	1	2	3	4	5	6	7	8	9	10	t_0 (mm)
Buckling design[1]	θ°	20.5	24.4	35.0	45.7	52.8	57.3	60.7	64.2	66.9	68.4	0.184
Buckling/DT design[1]	θ°	20.0	20.0	20.2	28.2	32.0	45.5	57.6	75.9	83.9	86.0	0.254
	±45º	Yes	Yes	Yes	Yes	Yes	No	No	No	No	No	-

[1]Note that the stacking sequence for the optimum bucking design is $[\theta/\text{-}\theta/\text{-}\theta/\theta/\text{-}\theta/\theta/\theta/\text{-}\theta]_s$ whereas for the buckling/DT optimum design it is $[\theta/\text{-}\theta/\text{-}\theta/\theta/\text{-}\theta/\theta/\theta/\text{-}\theta]$.

covered with ±45º plies. The 3 strips close to the panel edges with $\theta_i < 45°$ were initially covered by ±45º plies. The initial optimum results showed that the adjacent strips with $\theta_i < 45°$ were not covered by ±45º plies. Therefore, more ±45º plies were added until the strips with fiber angle $\theta_i < 45°$ were all covered by the ±45º plies. It can be seen that there are 5 strips requiring the addition of ±45º plies, see Table 1 for the fiber angles of the final optimum buckling/DT design. As the thickest tow in strip 1 is 0.742 mm, just below 0.75 mm, the stacking sequence consists of the original 8 plies.

Table 3 Comparison of panel mass and strains for optimum buckling design and buckling/DT design.

	Panel mass (kg)	Buckling strain (με)	DT strain (με)
Buckling design	1.34	6061	3682
Buckling/DT design	1.26	4588	6298

It is interesting to note the optimum buckling/DT design is 6% lighter than the buckling design, see Table 3. The buckling strain of the buckling/DT design is 4588 microstrain making it stiffer than the buckling design, which has a buckling strain of 6061 microstrain. The threshold strains for the buckling/DT optimum design were checked and the lowest threshold strain of 6298 microstrain occurs in strip 5 with a fiber angle of 32.0° at the third ply level and delamination diameter d = 30 mm. In comparison with the optimum buckling design, the damage tolerant strength improves by 71% from 3682 microstrain to 6298 microstrain.

In addition, the total bucking/DT laminate has a tensile transverse strain ε_y = 4947 microstrain in Strip 5 when the compressive design load 250kN is applied. The threshold strains at the first and third ply interfaces obtained with this transverse strain are around 8800 and 20000 mircostrain respectively. This proves that the assumption made in Section 3 with $\varepsilon_y = 0$ gives conservative values of sublaminate buckling strain ε^C and threshold strain ε_{th}.

6 Concluding Remarks and Future Work

A combined optimization strategy for minimum weight design of CTS panels satisfying buckling and DT constraints is developed. An efficient analytical CAI model is applied to provide the threshold strain for propagation of delamination.

Surface ±45º plies are studied in terms of their damage tolerance and buckling capacity, showing that such plies display good compromise between strength and buckling load. A buckling optimized CTS laminate and a buckling/DT optimum laminate are compared in terms of panel mass, fiber angles and DT strength. The results demonstrate that by re-optimizing fiber angles with a DT constraint, the damage tolerant strength improves by 71% with a 6% weight saving.

In future work, the design method will be applied to stiffened structures and sandwich panels.

Acknowledgements

The first author is supported by EPSRC (EP/H026371/1), GKN Aerospace and Airbus. VICONOPT is used with the permission of Cardiff University. The authors acknowledge the ABBSTRACT2 project team, especially Dr. Byung Chul Kim (University of Bristol) for developing the novel CTS technique.

References

[1] W. Liu and R. Butler "Buckling optimization of variable angle tow panels using the infinite strip method". *AIAA Journal*, doi:10.2514/1.J0521232013, 2013.

[2] M.W. Hyer, and R.F. Charette "The use of curvilinear fiber format in composite structure design". *AIAA paper* no. 1989-1404, 1989.

[3] Z. Gürdal, B.F. Tatting, C.K. Wu "Variable stiffness composite panels: Effects of stiffness variation on the in-plane and buckling response". *Composites Part A: Applied Science and Manuf*acturing, Vol. 39 no.5, pp. 911-922, 2008.

[4] E. Lund "Buckling topology optimization of laminated multi-material composite shell structures". *Composite Structures*, Vol. 91, pp. 158-167, 2009.

[5] A.W. Blom, M.M. Abdalla and Z. Gürdal "Optimization of course locations in the fiber-placed panels for general fiber angle distributions". *Composites Science and Technology*, Vol. 70, pp. 564-570, 2010.

[6] A.W. Blom "Structural performance of fiber-placed variable-stiffness composite conical and cylindrical shells". *PhD Thesis*, University of Delft, Holland, 2010.

[7] B.C. Kim, K. Potter and P.M. Weaver "Continuous tow shearing for manufacturing variable angle tow composites". *Composites Part A: Applied Science and Manufacturing*, Vol. 43, pp. 1347-1356, 2012.
[8] C.S. Lopes, P.P. Camanhob, Z. Gürdal, P. Maimí and E.V. González "Low-velocity impact damage on dispersed stacking sequence laminates. Part II: Numerical simulations". *Composites Science and Technology*, Vol. 69, pp. 937-947, 2009.
[9] A.T. Rhead, R. Butler, W. Liu, B.C. Kim and S.R. Hallett "Compression after impact strength of a buckling resistant, tow steered panel". ICCM19, Montreal, Canada, 2013.
[10] R. Butler, A.T. Rhead, W. Liu and N. Kontis "Compressive strength of delaminated aerospace Composites". *Philosophical Transactions of the Royal Society A*, Vol. 370, pp. 1759-1779, 2012.
[11] W.H. Wittrick and F.W. Williams "Buckling and vibration of anisotropic or isotropic plate assemblies under combined loadings". *International Journal of Mechanical Sciences*, Vol. 16, pp. 209-239, 1974.
[12] N. Baker, R. Butler and C.B. York "Damage tolerance of fully orthotropic laminates in compression". *Compos Science and Technology*, Vol. 72, pp. 1083-1089, 2012.
[13] A.T. Rhead, R. Butler and N. Baker "Analysis and compression testing of laminates optimised for damage tolerance". *Applied Composite Materials*, in press, doi:10.1007/s10443-010-9153-z, 2013.
[14] R. Butler and F.W. Williams "Optimum design using VICONOPT, a buckling and strength constraint program for prismatic assemblies of anisotropic plates". *Computers and Structures*, Vol. 43, No. 4, pp. 699–708, 1992.
[15] A.T. Rhead, R. Butler, W. Liu and N. Baker "The influence of surface ply fibre angle on the compressive strength of composite laminates containing delamination". *Aeronautical Journal*, Vol. 116, No. 1186, pp. 1313-1330, 2013.